



Paper Type: Original Article

Seismic Pounding Control of Adjacent Buildings Using MR Dampers: A Semi-Active Control Strategy

Mahdieh Zayyen Karin^{1*}, Hamid Reza Rabieifar²

¹ Department of Civil Engineering, Academic Center for Education, Culture and Research (ACECR), Rasht, Iran; mzkcivil64@gmail.com.

² Department of Civil Engineering, South Tehran Branch, Islamic Azad University, Tehran, Iran.

Citation:

Received: 20 July 2025

Revised: 01 September 2025

Accepted: 14 December 2025

Zayyen Karin, M., & Rabiei Far, H. R. (2026). Seismic pounding control of adjacent buildings using MR dampers: A semi-active control strategy. *Journal of civil aspects and structural engineering*, 3(2), 76–89.

Abstract

Pounding between adjacent buildings due to out-of-phase vibrations during earthquakes causes severe structural damage. This paper investigates the effectiveness of Magneto-Rheological (MR) dampers as semi-active control devices to mitigate seismic response and pounding risk between adjacent 10-story and 20-story buildings. The connected buildings are modeled as linear shear frames with identical floor levels. A Bouc-Wen-based modified model simulates the MR damper behavior, and an Linear Quadratic Regulator (LQR) controller computes the desired control force. An inverse MR damper model determines the command voltage. The system is subjected to near-fault (Kobe 1995) and far-fault (El Centro 1940) ground motions. Results show that MR dampers significantly reduce story displacements, drifts, and required separation distance (by ~22 cm for Kobe). Placing dampers only at the top two shared floors achieves 80% cost reduction with negligible performance loss compared to full installation. The study provides practical guidelines for economical pounding mitigation.

Keywords: Pounding control, Magneto-rheological damper, Semi-active control, Adjacent buildings, Seismic response.

1 | Introduction

Earthquakes cause over 780,000 deaths per decade and billions in economic losses. Among various failure modes, pounding between closely spaced adjacent buildings—due to different dynamic properties (mass, stiffness, period)—is a major cause of local and global collapse [1]. Urban land prices often force insufficient separation gaps, making pounding inevitable during strong ground motions.

Seismic codes (e.g., Iranian Standard 2800, UBC, EC8) prescribe minimum separation distances, but retrofitting existing dense urban fabrics is challenging. Researchers have proposed passive [2], active [3], semi-active [4], and hybrid control strategies [5] to interconnect adjacent buildings. Magneto-Rheological (MR) dampers—semi-active devices that change viscosity under a magnetic field—offer low power consumption,

✉ Corresponding Author: mzkcivil64@gmail.com

doi <https://doi.org/10.48314/jcase.v3i2.79>



Licensee System Analytics. This article is an open access article distributed under the terms and conditions of the Creative Commons Attribution (CC BY) license (<http://creativecommons.org/licenses/by/4.0>).

fast response, and fail-safe operation [6]. This study builds on Bharti et al. [7] and Dumne and Shrimali [8] by:

- I. Optimizing MR damper placement (full vs. partial floors).
- II. Using an Linear Quadratic Regulator (LQR) [9] + inverse MR model for voltage control [10].
- III. Comparing near-fault (Kobe) and far-fault (El Centro) excitations [11].
- IV. Quantifying cost-performance trade-offs.

2 | System Modeling and Equations of Motion

2.1 | Structural Model

Two adjacent buildings (10 stories and 20 stories) are modeled as 2D linear shear frames with identical floor levels. Only translational Degree of Freedoms (DOFs) per floor are considered. Mass and stiffness matrices are selected to obtain fundamental periods of 1.04 s (10-story) and 2.04 s (20-story) as per Bharti et al. [7]. Rayleigh damping with 5% damping ratio is assumed.

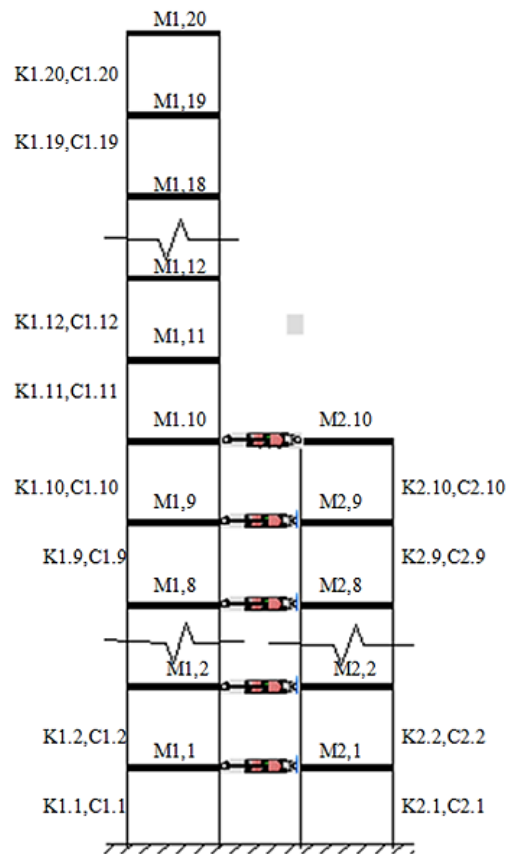


Fig. 1. Geometric model of two adjacent buildings (10 and 20 stories) with MR dampers at shared floor levels.

2.2 | Equations of Motion

Uncontrolled system:

$$[M]\{\ddot{u}\} + [C]\{\dot{u}\} + [K]\{u\} = -[M]\{r\}\ddot{u}_g. \quad (1)$$

Controlled system (with MR dampers):

$$[M]\{\ddot{u}\} + [C]\{\dot{u}\} + [K]\{u\} = -[M]\{r\}\ddot{u}_g + [D]\{f_{MR}\}, \tag{2}$$

where:

- I. $[M], [C], [K]$ = mass, damping, stiffness matrices (combined system).
- II. $\{u\}$ = relative displacement vector.
- III. \ddot{u}_g = ground acceleration.
- IV. $[D]$ = damper location matrix.
- V. $\{f_{MR}\}$ = MR damper force vector.

2.3 | Magneto-Rheological Damper Model (Modified Bouc-Wen)

The modified Bouc-Wen model [12] predicts MR damper force:

$$f = c_0\dot{x} + \alpha z + k_0x + k_1(x - x_0), \tag{3}$$

with evolutionary variable z governed by

$$\dot{z} = -\gamma |\dot{x}| z |z|^{n-1} - \beta \dot{x} |z|^n + A\dot{x}. \tag{4}$$

All parameters are voltage-dependent.

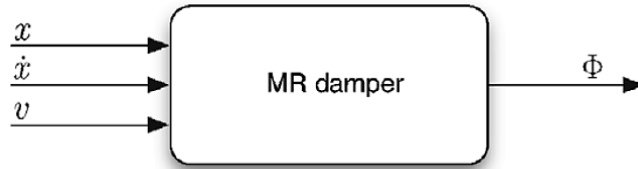


Fig. 2. Input/output variables of MR damper (displacement, velocity, voltage → force).

3 | Semi-Active Control Strategy

An LQR optimal controller computes the desired control force $\{f_{des}\}$ based on state feedback. The command voltage for each MR damper is obtained from an inverse model.

$$V = \frac{f_{des} - f_{min}}{f_{max} - f_{min}}, \tag{5}$$

where f_{min}, f_{max} are damper forces at 0V and 1V, respectively. Voltage is clipped to $[0 \cdot 1]$.

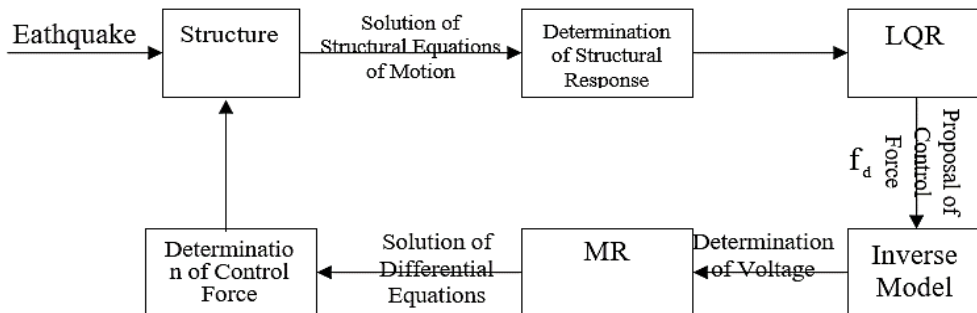


Fig. 3. Semi-active control algorithm flowchart.

Two placement strategies are evaluated:

Case 1. MR dampers at all shared floors (10 levels).

Case 2. MR dampers only at top two shared floors (floors 9 and 10) – 80% reduction in number of dampers.

4 | Numerical Simulation and Results

Ground motions:

- I. Near-fault: Kobe 1995 (PGA $\sim 0.82g$).
- II. Far-fault: El Centro 1940 (PGA $\sim 0.35g$).

Simulation performed in MATLAB/Simulink. Key response metrics: roof displacement, inter-story drift, floor acceleration, and relative displacement at the highest shared floor (pounding indicator).

4.1 | Near-Fault Excitation (Kobe 1995)

Case 1. MR dampers at All shared floors.

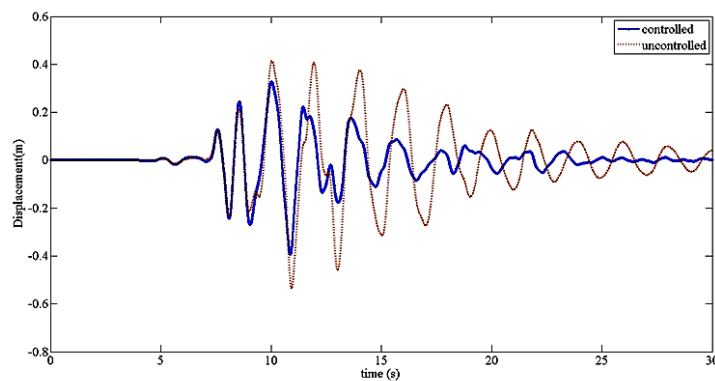


Fig. 4. Roof displacement – 20-story building (Kobe, Case 1).

→ Displacement reduced by $\sim 30\%$ compared to uncontrolled.

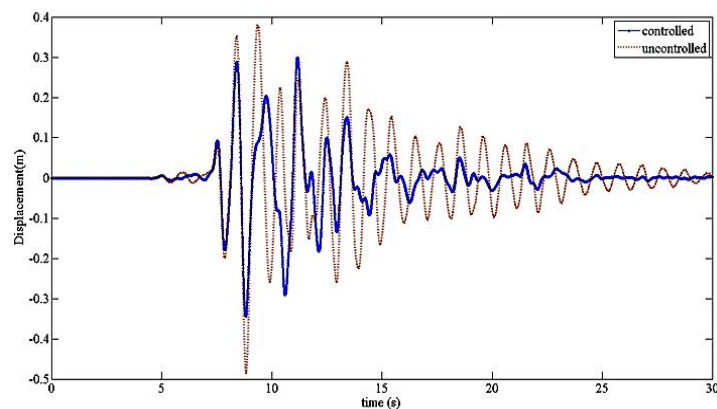


Fig. 5. Roof displacement – 10-story building (Kobe, Case 1).

→ Shorter building shows better response reduction.

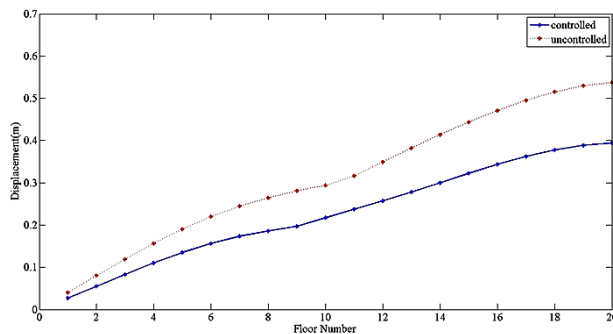


Fig. 6. Peak story displacement – 20-story (Kobe, Case 1).

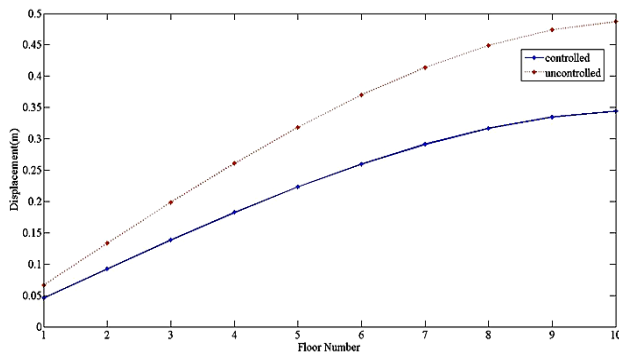


Fig. 7. Peak story displacement – 10-story (Kobe, Case 1).

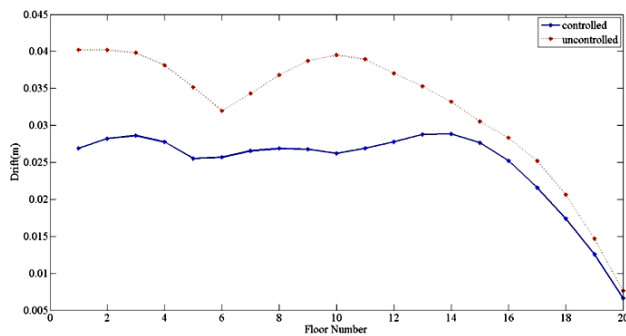


Fig. 8. Peak inter-story drift – 20-story (Kobe, Case 1).

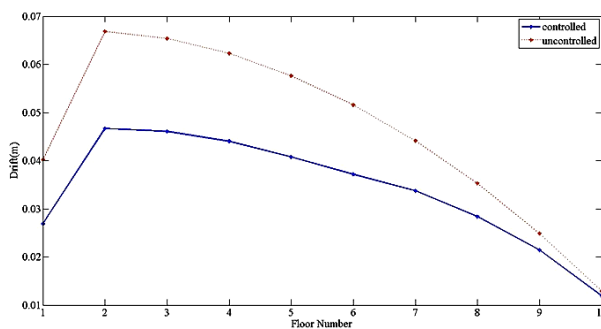


Fig. 9. Peak inter-story drift – 10-story (Kobe, Case 1).

→ Drifts reduced across all stories.

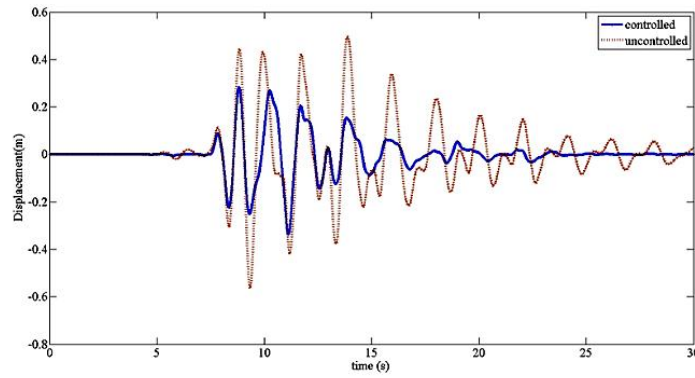


Fig. 10. Relative displacement at highest shared floor (Kobe, Case 1).

→ Required separation distance drops from 49.5 cm (uncontrolled) to 28.8 cm (controlled) → ~21 cm reduction.

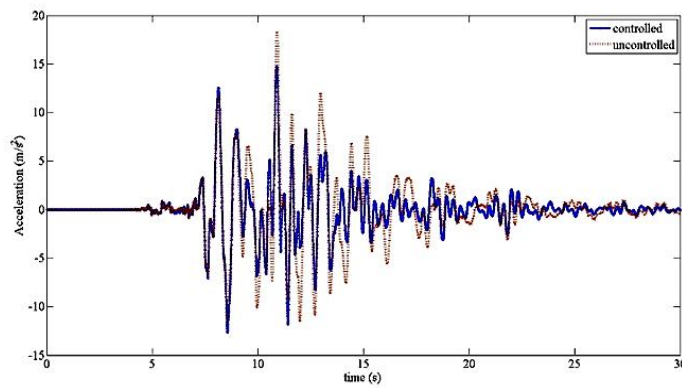


Fig. 11. Roof accelerations – both buildings.

→ Accelerations slightly increase in some cases due to added damping forces.

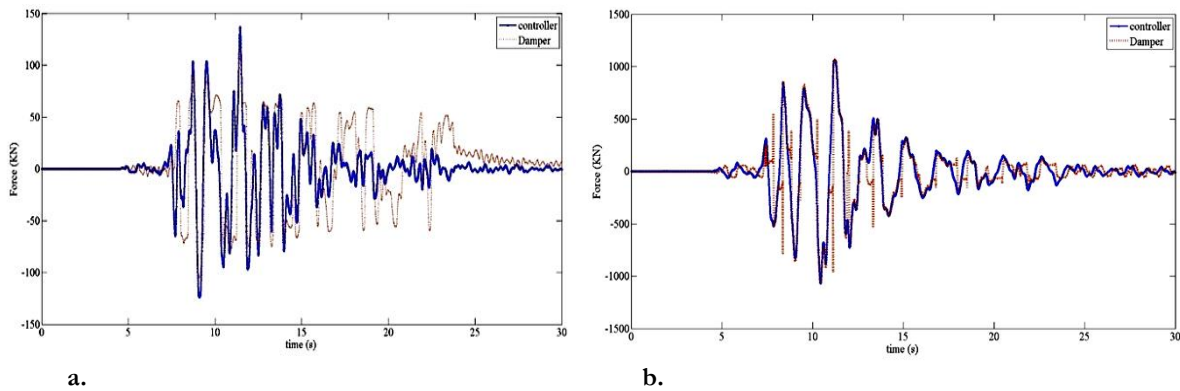


Fig. 12. LQR vs. MR force comparison and command voltages.

→ Good tracking at top floors; minimal voltage at lower floors suggests dampers act passively.

Case 2. MR dampers only at top two shared floors (9 and 10).

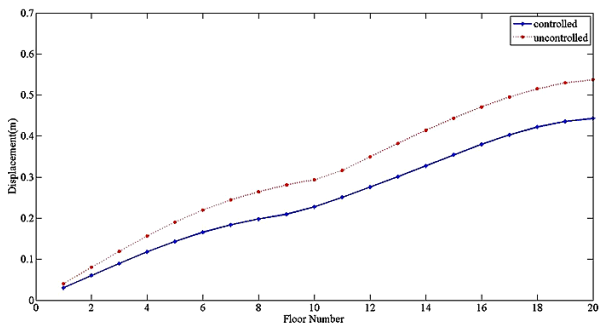


Fig. 13. Peak story displacement – 20-story (Kobe, Case 2).

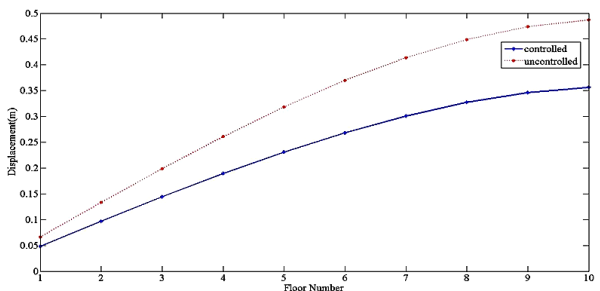


Fig. 14. Peak story displacement – 10-story (Kobe, Case 2).

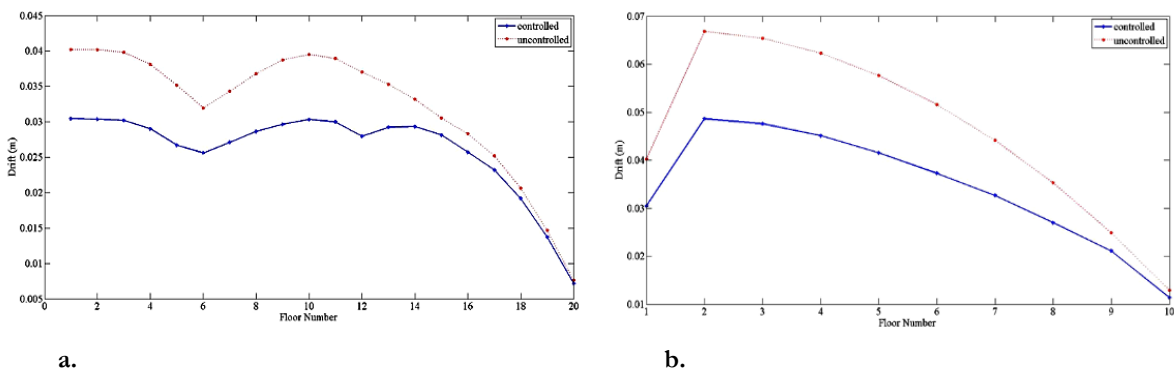


Fig. 15. Peak drift – both buildings (Case 2).

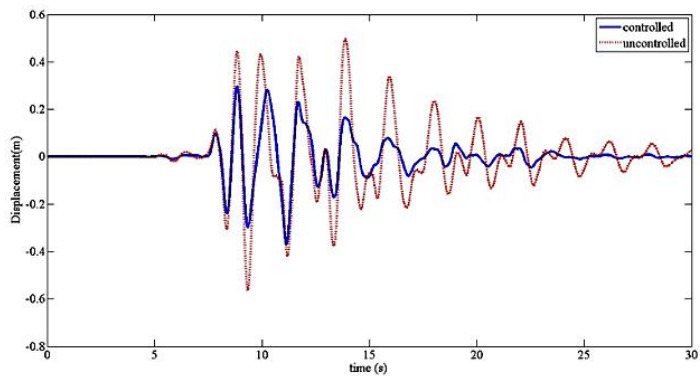


Fig. 16. Relative displacement at highest shared floor (Case 2).

→ Required separation: ~29.7 cm (only 1 cm more than Case 1).

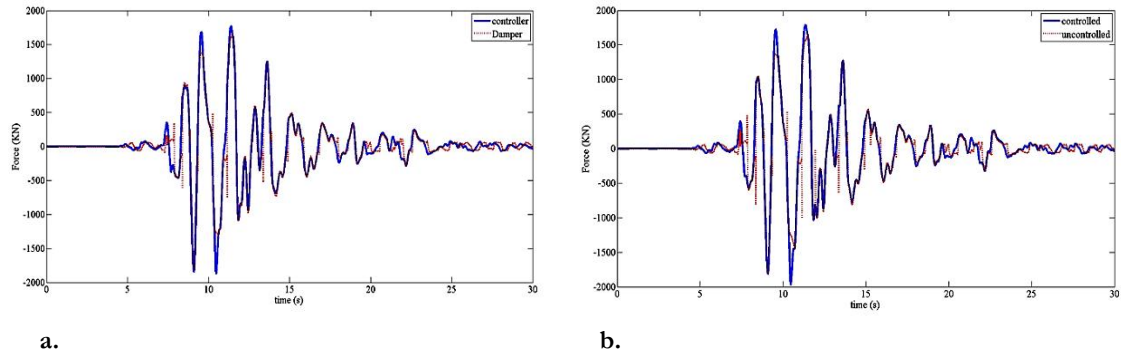


Fig. 17. Force tracking and voltage – floors 9 and 10.

→ Dampers now operate near full capacity (voltage $\sim 0.8\text{--}1.0$), indicating efficient use.

Conclusion for Kobe: Reducing dampers from 10 to 2 \rightarrow 80% cost saving, only 1 cm increase in required separation. Performance loss negligible.

4.2 | Far-Fault Excitation (El Centro 1940)

Case 1. MR dampers at all shared floors.

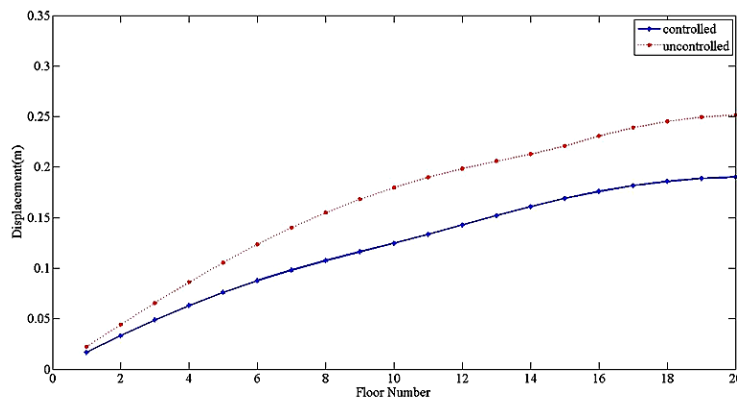


Fig. 18. Peak story displacement – 20-story (El Centro, Case 1).

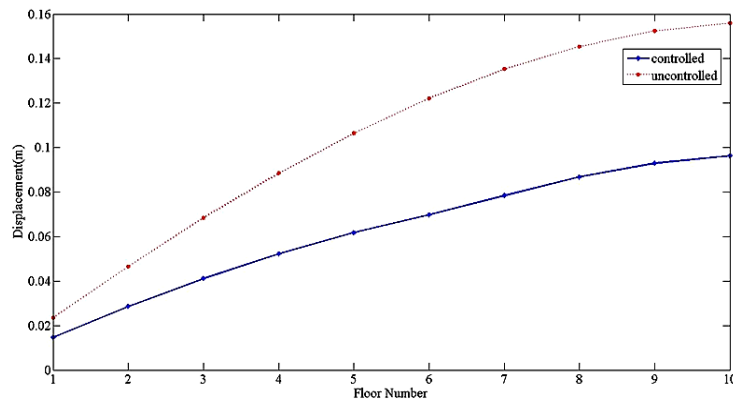


Fig. 19. Peak story displacement – 10-story (El Centro, Case 1).

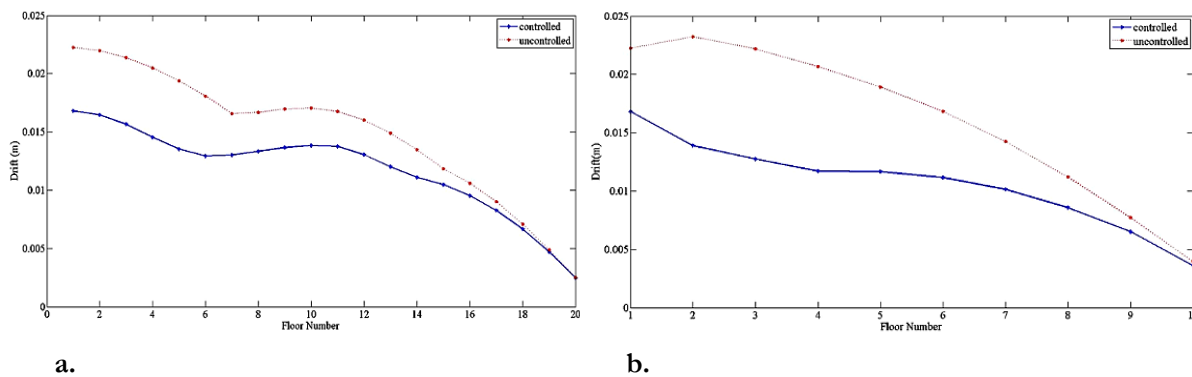


Fig. 20. Peak drift – both buildings.

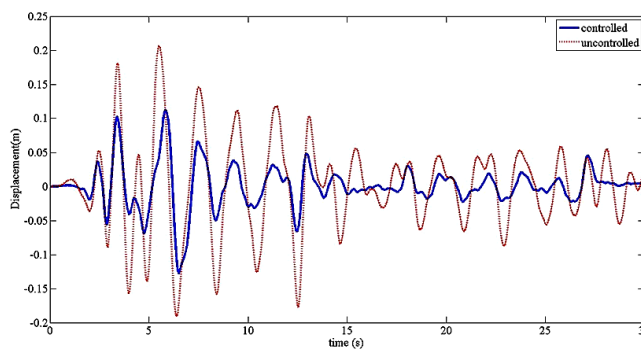


Fig. 21. Relative displacement at highest shared floor.

→ Required separation: 48.7 cm (uncontrolled) → 34.4 cm (controlled) → ~14 cm reduction.

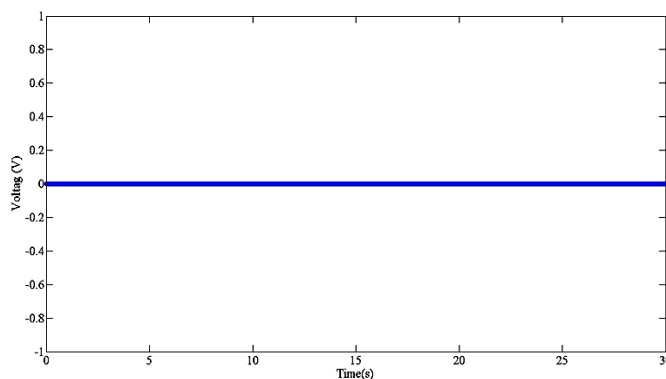


Fig. 22. Force tracking and voltage.

→ Lower floors generate near-zero voltage → passive behavior → inefficient.

Case 2. MR dampers only at top two shared floors.

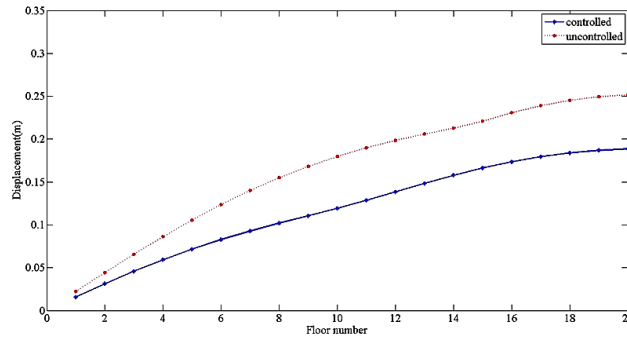


Fig. 23. Peak story displacement – 20-story (El Centro, Case 2).

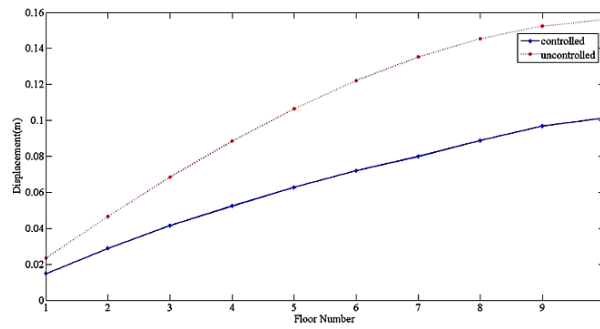


Fig. 24. Peak story displacement – 10-story (El Centro, Case 2).

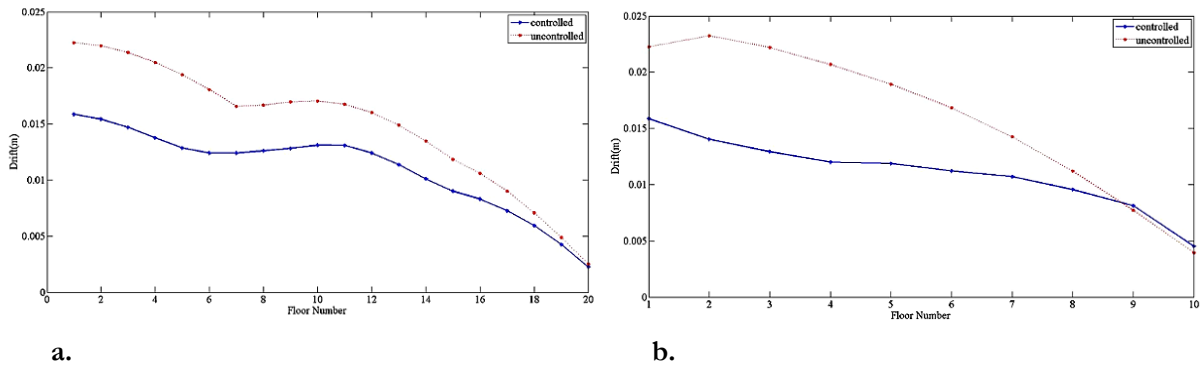


Fig. 25. Peak drift – both buildings.

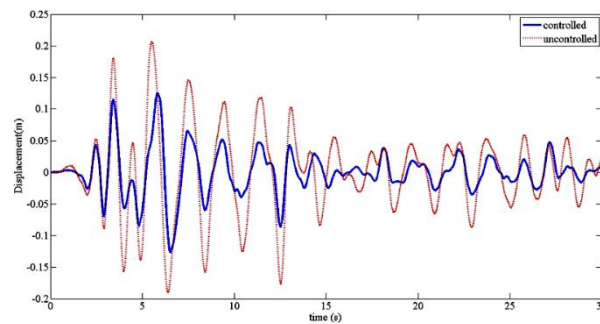


Fig. 26. Relative displacement at highest shared floor.

→ Required separation: 29.7 cm (slightly better than Case 1 for El Centro).

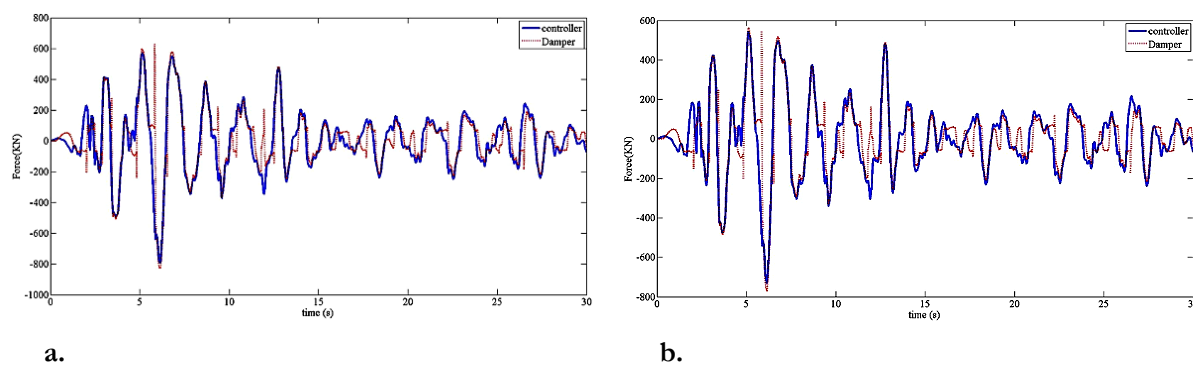


Fig. 27. Force tracking and voltage – floors 9 and 10.

→ Dampers operate at higher voltage, better tracking, and improved response reduction compared to Case 1.

Conclusion for El Centro: Full damper installation at all floors is inefficient (lower floors inactive). Two dampers at top floors give superior or equal performance.

5 | Validation with Literature

Comparison with Bharti et al. [7] – same building models but different control algorithm (Lyapunov vs. LQR) and voltage range (0–3V in reference).

Table 1. Comparison table – uncontrolled, Case 1, Case 2, and reference results.

Location / Response	Uncontrolled	Case 1 (All Floors)	Case 2 (Only Floors 9 and 10)	Reference (2) (All Floors, Lyapunov, 3V)
20-story building – Roof displacement (cm)	53.68	39.43	49.28	48.68
10-story building – Roof displacement (cm)	48.68	34.43	35.64	39.43
20-story building – Peak inter-story drift (cm)	1.29	1.19	1.13	1.27
10-story building – Peak inter-story drift (cm)	0.76	0.66	0.71	0.97
20-story building – Peak floor acceleration (g)	1.86	1.50	1.76	2.50
10-story building – Peak floor acceleration (g)	1.27	0.97	1.13	1.86
Required separation distance at highest shared floor (cm)	49.49	28.76	29.70	28.76

Key validation results (Kobe, Case 2 vs. reference):

- I. Roof displacement (20-story): 35.6 cm (present) vs. 39.4 cm (ref.) → slightly better.
- II. Roof displacement (10-story): 49.3 cm (present) vs. 53.7 cm (ref.) → comparable.
- III. Required separation: 29.7 cm (present) vs. 28.8 cm (ref.) → very close.

Discrepancy source: Different control law (LQR vs. Lyapunov) and voltage limit (1V vs. 3V). LQR with inverse model performs well even with limited voltage.

6 | Conclusion

- I. MR dampers effectively reduce pounding risk in adjacent 10- and 20-story buildings under both near-fault and far-fault earthquakes.
- II. Required separation distance can be reduced by 21–22 cm (Kobe) and 14–19 cm (El Centro), allowing denser urban construction without compromising safety.
- III. Full damper installation at all shared floors is not necessary. Lower-floor dampers often operate passively (near-zero voltage) and may even reduce upper damper efficiency.

IV. Placing MR dampers only at the top two shared floors (80% fewer devices) achieves:

- Negligible performance loss (≤ 1 cm increase in required separation).
- Improved voltage utilization (0.8–1.0 vs. 0–0.3).
- Better LQR-MR force tracking.

V. Shorter building (10-story) consistently experiences better response reduction than the taller building (20-story).

VI. Increasing voltage reduces displacement but may increase acceleration – a trade-off that requires careful tuning.

Acknowledgments

The authors would like to express their sincere appreciation to all colleagues and experts who provided valuable technical insights and support throughout this research.

Conflicts of Interest

The authors declare that they have no known competing financial interests or personal relationships that could have appeared to influence the work reported in this paper.

Data Availability

All data generated or analyzed during this study are included in this published article. Additional data supporting the findings of this study are available from the corresponding author upon reasonable request.

Authors' Contributions

M.Z.K.: Conceptualization, Methodology, Software, Formal Analysis, Investigation, Data Curation, Visualization, Writing—Original Draft Preparation.

H.R.R.: Validation, Supervision, Writing—Review and Editing, Technical Guidance, Project Administration.

All authors have read and agreed to the published version of the manuscript.

Funding

This research received no external funding.

Consent for Publication

All authors have read and approved the final version of the manuscript and consent to its publication.

Ethics Approval and Consent to Participate

This study did not involve human participants or animals. Therefore, ethics approval and informed consent to participate were not required.

References

- [1] Anagnostopoulos, S. A. (1995). Earthquake induced pounding: State of the art. *Proceedings of the 10th european conference on earthquake engineering* (pp. 897–905). Balkema: Rotterdam.
- [2] Xu, Y. L., He, Q., & Ko, J. M. (1999). Dynamic response of damper-connected adjacent buildings under earthquake excitation. *Engineering structures*, 21(2), 135–148. [https://doi.org/10.1016/S0141-0296\(97\)00154-5](https://doi.org/10.1016/S0141-0296(97)00154-5)

- [3] Zou, L., Huang, K., Wang, L., Butterworth, J., & Ma, X. (2012). Vibration control of adjacent buildings considering pile-soil-structure interaction. *Journal of vibration and control*, 18(5), 684–695. <https://doi.org/10.1177/1077546311408989>
- [4] Ni, Y. Q., Ko, J. M., & Ying, Z. G. (2001). Random seismic response analysis of adjacent buildings coupled with non-linear hysteretic dampers. *Journal of sound and vibration*, 246(3), 403–417. <https://doi.org/10.1006/jsvi.2001.3679>
- [5] Pourzeynali, S., Lavasani, H. H., & Modarayi, A. H. (2007). Active control of high rise building structures using Fuzzy logic and genetic algorithms. *Engineering structures*, 29(3), 346–357. <https://doi.org/10.1016/j.engstruct.2006.04.015>
- [6] Yang, G., Spencer, B. F., Carlson, J. D., & Sain, M. K. (2002). Large-scale MR fluid dampers: Modeling and dynamic performance considerations. *Engineering structures*, 24(3), 309–323. [https://doi.org/10.1016/S0141-0296\(01\)00097-9](https://doi.org/10.1016/S0141-0296(01)00097-9)
- [7] Bharti, S. D., Dumne, S. M., & Shrimali, M. K. (2010). Seismic response analysis of adjacent buildings connected with MR dampers. *Engineering structures*, 32(8), 2122–2133. <https://doi.org/10.1016/j.engstruct.2010.03.015>
- [8] Dumne, S. M., & Shrimali, M. K. (2007). Earthquake performance of isolated buildings connected with MR dampers. *Proceedings of the 8th pacific conference on earthquake engineering, singapore, paper* (pp. 1-10). National Technological University (NTU), Singapore. <https://www.researchgate.net/publication/316583712>
- [9] Hossain, M. A., Azim, M. I., Mahmud, M. A., & Pota, H. R. (2015). Primary voltage control of a single-phase inverter using linear quadratic regulator with integrator. *2015 australasian universities power engineering conference (AUPEC)* (pp. 1–6). IEEE. <https://doi.org/10.1109/AUPEC.2015.7324843>
- [10] Tanaka, R., Inoue, S., Shibasaki, H., Ogawa, H., Murakami, T., & Ishida, Y. (2015). An approach to model-following controller design based on a stabilized digital inverse system. *Proceedings of the institution of mechanical engineers, Part I: Journal of systems and control engineering*, 229(9), 829–837. <https://doi.org/10.1177/0959651815585210>
- [11] Chopra, A. K., & Chintanapakdee, C. (2001). Comparing response of SDF systems to near-fault and far-fault earthquake motions in the context of spectral regions. *Earthquake engineering & structural dynamics*, 30(12), 1769–1789. <https://doi.org/10.1002/eqe.92>
- [12] Bahar, A., Pozo, F., Acho, L., Rodellar, J., & Barbat, A. (2010). Hierarchical semi-active control of base-isolated structures using a new inverse model of magnetorheological dampers. *Computers & structures*, 88(7), 483–496. <https://doi.org/10.1016/j.compstruc.2010.01.006>